East European Journal of Physics. 3. 416-424 (2024)
DOI:10.26565/2312-4334-2024-3-50 ISSN 2312-4334

STRENGTHEN THE POWER CONVERSION EFFICIENCY OF SOLAR CELL BASED $RbGeI_3$: NUMERICAL APPROACH

Lazhar Loumachi[a], Abderrahim Yousfi[b]*, Okba Saidani[b], Abdullah Saad Alsubaie[c], Oussama Abed[b], Samir Amiri[b], Girija Shankar Sahoo[d], Md. Rasidul Islam[e]

[a]*Department of Civil Engineering, Faculty of sciences and technology, University Mohamed El Bachir El Ibrahimi of Bordj Bou Arréridj-34030, Algeria*
[b]*ETA Laboratory, Department of electronics, Faculty of sciences and technology, University Mohamed El Bachir El Ibrahimi of Bordj Bou Arréridj-34030, Algeria*
[c]*Department of Physics, College of Khurma University College, Taif University, Taif 21944, Saudi Arabia*
[d]*School of Electronics Engineering (SENSE), Vellore Institute of Technology, Vandalur Kellambakkam Road, Chennai, Tamil Nadu 600127, India*
[e]*Department of Electrical and Electronic Engineering, Bangamata Sheikh Fojilatunnesa Mujib Science & Technology University, Jamalpur, 2012, Bangladesh*
**Corresponding Author e-mail: abderrahim.yousfi@univ-bba.dz; lazhar.loumachi@univ-bba.dz*
Received May 1, 2024; revised June 12, 2024; accepted June 20, 2024

The current study employs numerical simulations via the SCAPS-1D platform to investigate the performance of solar cells based on perovskite, with $RbGeI_3$ utilized as an absorber material possessing a wide bandgap of 1.31 eV. Through systematic exploration of various parameters including temperature, layer thickness, doping, and defects, the study aims to enhance the efficiency of the solar cells, considering their sensitivity to temperature variations. Results demonstrate that the proposed configuration effectively extends the absorption spectrum into the near-infrared region, with the thickness of the $RbGeI_3$ layer emerging as a critical factor influencing device performance. Analysis reveals that the series resistance peaks at 2 $\Omega \cdot см^2$, while the shunt resistance achieves optimal output parameters of up to 10^3 $\Omega \cdot см^2$. Moreover, optimization efforts yield a solar cell exhibiting a power conversion efficiency of 24.62%, fill factor of 82.8%, open circuit voltage of 0.99V, and short circuit current density of 33.20 mA/cm^2 at a $RbGeI_3$ thickness of 0.6 um. This comprehensive numerical investigation not only enhances understanding of the intricate factors influencing perovskite solar cells but also suggests promising avenues for future advancements in the field.
Keywords: *Solar cell; $RbGeI_3$; SCAPS-1D; PSC; PCE*
PACS: 84.60. Jt, 88.40.jm

1. INTRODUCTION

Perovskite solar cells (PSCs) have emerged as a rapidly advancing technology within the photovoltaics field, offering significant promise [1]. Named after their structure resembling the naturally occurring mineral perovskite, these solar cells typically feature an active layer comprising an organic-inorganic halide perovskite material [2-3]. This material exhibits exceptional light-harvesting capabilities and can be economically manufactured. Noteworthy advantages of PSCs include their high-power conversion efficiencies, cost-effectiveness in production [4], and potential for flexible and transparent applications [5]. However, challenges related to stability, toxicity (stemming from lead content in certain formulations), and scalability for large-scale commercial production persist [6-7]. Over recent years, the efficiency of organic-inorganic hybrid perovskites has notably increased, from 3.81% to 25.2% [8]. Researchers across various disciplines have devoted substantial efforts to enhancing PSC efficiency through optimizations of perovskite layers and refinement of device structures [9]. One avenue explored to address these challenges involves the incorporation of rubidium (Rb^+) into perovskite compositions, either as a dopant or additive [10-11]. Rubidium doping can modify the perovskite's properties, influencing its electronic structure and enhancing stability, a critical factor for commercialization [12]. Additionally, rubidium has been found to improve photovoltaic performance by enhancing power conversion efficiency and open-circuit voltage while reducing defects within the perovskite structure [13]. Efforts to develop environmentally friendly alternatives to lead-based perovskites have led to the investigation of germanium-based perovskites, such as $CsGeI_3$ [14]. Germanium-based perovskites offer tunable bandgaps, allowing for tailored electronic properties to optimize solar absorption [15-16]. Investigations into lead-free perovskites, including those containing germanium, focus on their stability under various environmental conditions, a crucial consideration for practical solar cell applications [17]. In perovskite solar cells, iodide ions are commonly utilized as integral components within the perovskite material, contributing significantly to light absorption and thereby playing a pivotal role in the photovoltaic conversion process [18]. The composition of halide ions influences both the bandgap and absorption characteristics of the perovskite material [19]. Rubidium, germanium, and triiodide each fulfill distinct roles in shaping the composition and structure of perovskite solar cells [20-21]. These elements exert influence over electronic properties, stability, and photovoltaic performance, offering avenues for researchers to tailor the characteristics of solar cells for optimal efficiency and stability [22].

Cite as: L. Loumachi, A. Yousfi, O. Saidani, A.S. Alsubaie, O. Abed, S. Amiri, G.S. Sahoo, Md.R. Islam, East Eur. J. Phys. 3, 416 (2024), https://doi.org/10.26565/2312-4334-2024-3-50

This study introduces an innovative approach to simulating solar cells using the SCAPS-1D simulator. Our method incorporates advanced electron transport layers (ETLs) comprising C_{60} and hole transport layers (HTLs) composed of CBTS. Simulation results reveal that solar cell heterostructures, specifically ITO/C_{60}/$RbGeI_3$/CBTS/Ag, demonstrate remarkably high photoconversion efficiency. Furthermore, our investigation extends beyond surface-level analysis, encompassing a comprehensive exploration of multiple parameters influencing the performance of $RbGeI_3$-based solar cells.

2. DEVICE SETTINGS AND SIMULATION PROCESS

The architecture of the solar cell employed in our study comprises three primary components: the electron transport layer (ETL), the perovskite layer doped with p-type material, and the hole transport layer (HTL). When illuminated by light, this configuration initiates the generation of excitons, which are particle pairs confined within the energy state, primarily within the perovskite layer [23]. These excitons, consisting of electrons and holes, possess relatively extensive diffusion lengths, facilitating their migration into the p-region (for electrons) or n-region (for holes) [24-25]. At the interface between the ETL and the perovskite layer, the excitons (electron-hole pairs) undergo separation. Subsequently, electrons are transported through the ETL toward the respective electrode, while holes efficiently traverse the HTL [26]. The existence of a built-in electric field between the ETL (or HTL) and the perovskite layer promotes the dissociation of excitons and their subsequent transport. This electric field accelerates the movement of electrons and holes towards their corresponding contacts, thereby enhancing the overall efficiency of the solar cell [27]. In our simulations, we incorporated advanced materials for the ETL and HTL layers, specifically employing ceric dioxide (C_{60}) for the ETL and CBTS for the HTL [28]. Simulation outcomes revealed that solar cell structures comprised of indium tin oxide ITO/C_{60}/ $RbGeI_3$/CBTS/Ag exhibited notably high photoconversion efficiency, as depicted in Figure 1. The integration of these advanced materials contributes to the overall enhancement of solar cell performance.

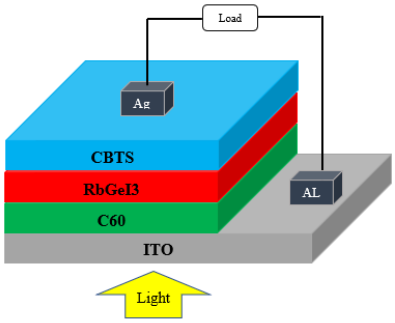

Figure 1. Design configuration of the $RbGeI_3$ based PSC

The simulations were conducted under standard operating conditions, utilizing AM1.5G light and an ambient temperature of 300 K. Moreover, as detailed in Tables 1, meticulous definition of input modeling parameters was undertaken for the hole transport layer (HTL), absorber layer ($RbGeI_3$), and electron transport layer (ETL) [29].

Table 1. Parameters of ETL, absorber and HTL

Parameters	ITO	ETL (C60)	PVK ($RbGeI_3$)	HTL (CBTS)
Thickness (µm)	0.5	0.1	0.4	0.05
Electron Affinity χ (eV)	4.1	3.9	3.9	3.6
Band gap Eg (eV)	3.5	1.31	1.31	1.9
Relative Permittivity εr	9	7.5	23.01	5.4
Effective Density of States (CB)	2.2×10^{18}	1×10^{19}	1.8×10^{18}	10^{19}
Effective Density of States (VB)	1.8×10^{18}	1×10^{19}	1×10^{18}	10^{19}
Electron Mobility µn(cm^2/Vs)	20	10^{-2}	28.6	200
Hole Mobility µp(cm^2/Vs)	10	10^{-2}	27.3	8.6×10^{3}
Acceptor Density NA(1/cm^3)	0	0	1×10^{15}	10^{18}
Donor Density ND (1/cm^3)	10^{21}	10^{18}	0	2
Defect Density Nt	10^{14}	10^{14}	1×10^{14}	10^{14}

The accurate representation and emulation of the solar cell's behavior and performance within the simulation framework necessitate careful consideration of these parameters. By employing SCAPS-1D numerical simulations, our understanding of the fundamental principles and mechanisms governing solar cells has been greatly enhanced. These simulations have identified the primary variables that exert the most significant impact on the performance of these devices [30]. Through numerical methods for solving carrier continuity equations and the one-dimensional Poisson equation, SCAPS-1D offers invaluable insights into the behavior of semiconductor materials under stable conditions. Specifically, the Poisson equation plays a crucial role in elucidating the relationship between space charge density and the electric field (E) across a p-n junction. Equation (1) aids in comprehending the semiconductor material utilized in solar cells, thereby deepening our understanding of electrostatics and charge distribution [31].

$$\left(\frac{\partial^2\psi}{\partial x^2}\right) = -\frac{\partial E}{\partial x} = -\frac{\rho}{\varepsilon_s} = -\frac{q}{\varepsilon_s}\left[p - n + N_d^+ - N_a^- + N_{def}\right]. \quad (1)$$

The carrier continuity equation in the device can be expressed as follows, where Ψ signifies the electrostatic potential, εs means the static relative permittivity, q is the charge, e and n explain respectively the electrons and holes, Nd^+ is the donor density, Na^- is the acceptor density, and N_{def} represents the defect density of both donor and acceptor [32-33].

$$-\frac{\partial j_p}{\partial x} + G - U_p(n,p) = 0, \quad (2)$$

$$-\frac{\partial j_n}{\partial x} + G - U_n(n,p) = 0. \quad (3)$$

The carrier current density can also be obtained using the following equation [34], where j_p and j_n signifies the hole and electron current densities, G is the carrier generation rate, and Un (n, p) and Up (n, P) are the rates at which electrons and holes recombine [35].

$$j_p = qn\mu_p E + qD_p\frac{\partial n}{\partial x}, \quad (4)$$

$$j_n = qn\mu_n E + qD_n\frac{\partial n}{\partial x}. \quad (5)$$

Simulations using SCAPS-1D allow the derivation values of short-current density (Jsc), power conversion efficiency (PCE), fill factor (FF) and open circuit voltage (V_{oc}) under varying thicknesses and temperatures [36]. where q denotes the charge, μp and μn represent carrier mobilities, and D_p, D_n are the diffusion coefficients [37]. These simulations may be performed in both lighted and dark environments, taking into account a range of temperatures, and they can be applied to seven different layers of the solar cell [38].

3. RESULTS AND DISCUSSION

3.1. Influence of Absorber ($RbGeI_3$) thickness:

In this section, we delve into the proposed structure of solar cell-based perovskite, comprising the layers mentioned earlier, and break it down into several subsections. We commence with an exploration of thickness variation. Figure 2.a showcases the current density–voltage (J–V) characteristics of perovskite solar cells incorporating $RbGeI_3$.

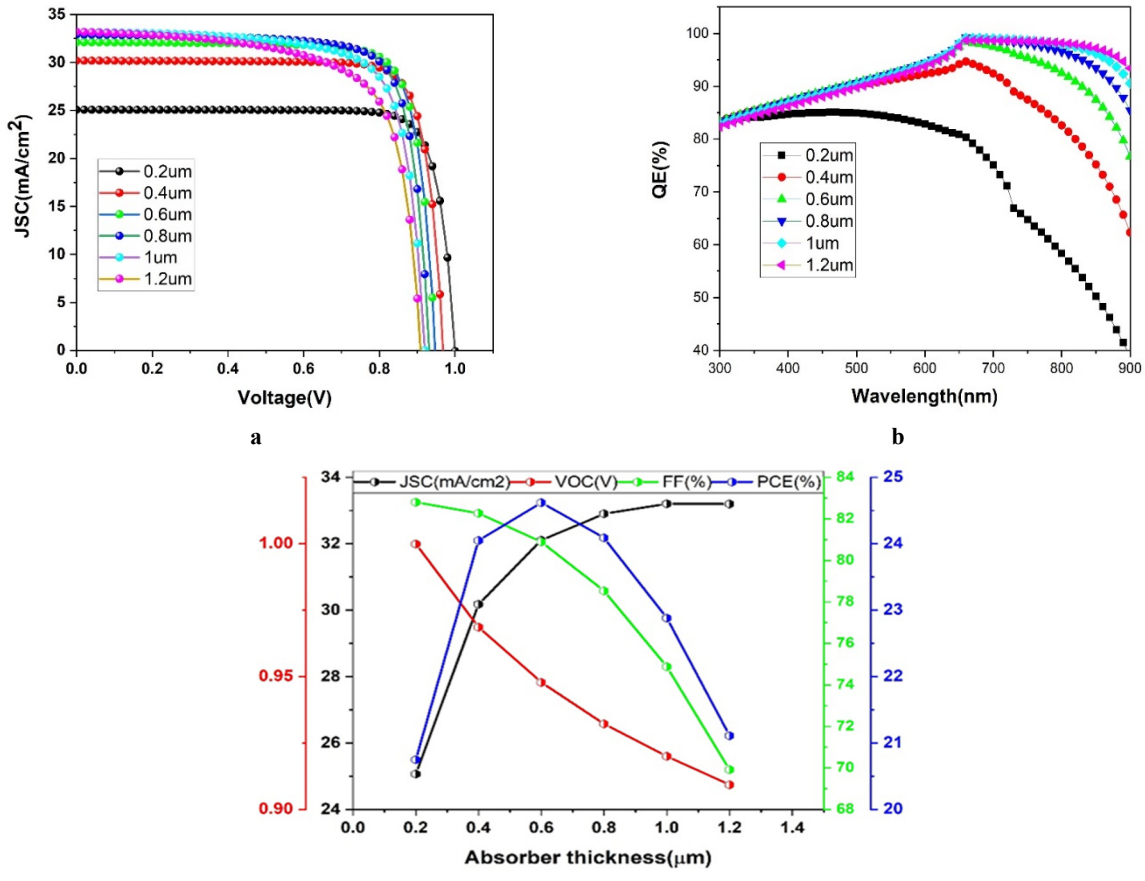

Figure 2. Effect of perovskite thickness on J–V (a), QE (b) and VOC, JSC, FF, PCE (c)

The thickness of the perovskite layer ($RbGeI_3$) was altered to assess its impact. It is observed that the short-circuit current density (J_{SC}) increases proportionally with absorber thickness, while the open-circuit voltage (V_{OC}) decreases, as illustrated in Figure 2.a. Figure 2.b displays the external quantum efficiency (QE) analysis, examining the effect of varying absorber thickness from 200 nm to 1200 nm across a wavelength range of 300 nm-900 nm. The QE of the structure significantly improves when the thickness of the RbGeI3 light harvester is below 0.6 µm, indicating a notable enhancement in absorption. However, the increase in QE diminishes when the thickness exceeds 0.6 µm, suggesting a less significant rise in absorption. With increasing $RbGeI_3$ film thickness, better absorption of longer wavelengths is observed. Short Circuit Current Density (J_{sc}) and Power Conversion Efficiency (PCE) are presented, showing an increase with the perovskite layer thickness, but a decrease at 0.6 µm thickness. A thinner perovskite layer boosts sunlight absorption, leading to higher open-circuit voltage and improved fill factor. However, this reduction in efficiency at 0.6 µm thickness is attributed to potential issues such as increased charge recombination, trapping, and non-uniformity within the perovskite layer [39]. Excessive thickness hampers charge extraction, negatively affecting overall solar cell efficiency. The solar cell yields a Jsc of 33.20 mA cm^{-2}, with a Voc of 0.99 V, FF of 82.8%, and Power Conversion Efficiency of 24.62%. Figure 2.c presents the Quantum Efficiency spectra for $RbGeI_3$ perovskite solar cells, revealing a substantial QE value exceeding 90% across a wide wavelength spectrum from 600 to 850 nm, with the photon spectral response extending to approximately 850 nm. The photocurrent densities derived from QE spectra align with the Jsc values obtained in J-V curves recorded under a solar simulator.

3.2. Influence of ETL Thickness

In perovskite solar cells, the electron transport layer (ETL) is pivotal for effectively extracting and conveying electrons generated during light absorption. Donor doping involves purposefully introducing dopant atoms that contribute electrons into the ETL material. Heavily donor-doping the electron transport layer in perovskite solar cells serves multiple critical functions: enhancing electron mobility within the ETL, which facilitates easier electron movement, diminishes recombination, and boosts overall efficiency [40]. Moreover, donor doping aids in establishing a favorable energy level alignment at the perovskite layer-ETL interface, thus aiding in efficient electron extraction and minimizing losses due to recombination. Additionally, it reduces energy barriers, facilitating smoother electron movement through the ETL, thereby improving charge transport efficiency and enhancing the stability of the perovskite solar cell over time. This precise tuning of energy levels within the ETL optimizes energy level alignment between different layers of the solar cell, leading to improved charge transport and reduced losses [41]. However, careful optimization is essential as excessive doping may result in undesirable effects such as increased carrier trapping or material instability. Factors such as choice of dopant, doping concentration, and specific characteristics of the perovskite material must be considered for effective enhancement of the ETL in perovskite solar cells [42]. As depicted in Figure 3.a, the current density–voltage (J–V) characteristics of the proposed configuration involving C_{60} are shown, varying its thickness to explore its impact on the solar cell. To enhance output performance, a thinner C_{60} layer is preferred, with optimal values observed at 0.4um thickness. Figure 3.b illustrates the impact of donor doping of the ETL on output performance. The device features a heavily doped C_{60} layer at a concentration of $10^{20}cm^{-3}$, resulting in J_{SC}=25.13 mA/cm^2, V_{OC}=1.00V, FF=83.09 %, and PCE=20.99%.

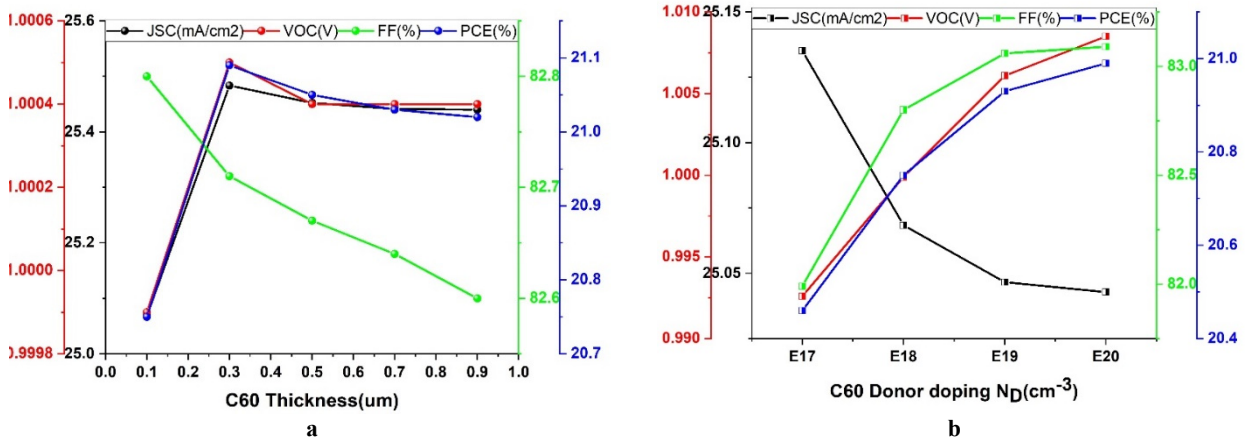

Figure 3. Effect of ETL thickness on V_{OC}, J_{SC}, FF, PCE for Donor doping N_D (a) and Thickness (b)

3.3. Influence of HTL Thickness

The thickness of the Hole Transport Layer (HTL) in a perovskite solar cell plays a crucial role in determining the device's performance. Various factors are at play in understanding how HTL thickness impacts perovskite solar cells. Firstly, optimal thickness is essential for efficient charge extraction from the perovskite layer, ensuring that holes can effectively reach the HTL and be collected at the electrode. Conversely, if the HTL is too thin, it may fail to adequately collect and transport holes, leading to increased recombination and decreased device efficiency. Additionally, increasing HTL thickness may elevate contact resistance between the HTL and the electrode, hindering charge carrier flow and

thereby diminishing electrical performance. Balancing thickness is therefore crucial to allow efficient charge transport while minimizing contact resistance. Moreover, the organic nature of the HTL may lead to light absorption, with thicker HTLs potentially reducing light reaching the perovskite layer, affecting device stability [43]. The compatibility between HTL material and the perovskite layer is vital for long-term stability, as HTL thickness influences energy level alignment at the interface. Optimization is necessary, considering different perovskite formulations and HTL materials, with trade-offs between charge transport optimization, fabrication ease, and cost. Experimental observations indicate that decreasing the thickness of the HTL layer enhances electron transfer properties, improving charge extraction and boosting short-circuit current density, consequently increasing energy conversion efficiency and open circuit voltage due to reduced recombination [44]. However, a decrease in Fill Factor is noted with thinner HTL layers. As presented in Figure 4, the solar cell exhibited a Power Conversion Efficiency (PCE) of 21.69 %, with a V_{oc} of 1.00 V, a Jsc of 26.08 mA cm^{-2}, and an FF of 82.93%.

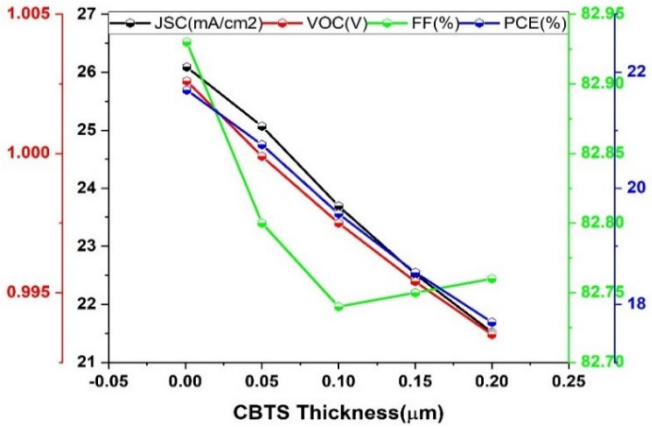

Figure 4. Effect of HTL thickness on V_{OC}; J_{SC}; FF; PCE

3.4. Influence of Defect Absorber

The presence of defects within the perovskite absorber layer of a perovskite solar cell profoundly influences both its performance and stability. Various factors come into play regarding the impact of these defects on the perovskite layer. Firstly, defects can serve as recombination centers, facilitating the recombination of electron-hole pairs generated by light absorption. This recombination process diminishes the cell's overall efficiency by limiting the number of charge carriers available for generating electric current. Additionally, defects can introduce trap states within the perovskite material's bandgap, capturing and temporarily immobilizing charge carriers, thereby delaying recombination and affecting charge carrier transport [45]. These trap states create energetic barriers for charge carriers, impacting their mobility and contributing to non-radiative recombination. The presence of defects also leads to a decrease in the open-circuit voltage (V_{oc}) of the solar cell by introducing additional energy levels that hinder charge carrier separation and extraction, thus affecting the fill factor (FF) as well, which measures the device's utilization of generated electrical current [46]. Moreover, defects contribute to the degradation of the perovskite material over time, especially under exposure to moisture, heat, or light, leading to decreased device performance and stability. In Figure 5, the performance characteristics of the defect absorber are examined to understand its impact, showing a decrease in short-circuit current density (J_{sc}), open-circuit voltage (V_{oc}), fill factor (FF), and power conversion efficiency (PCE) with increasing defect density. The solar cell exhibited a PCE of 23.14%, with a V_{oc} of 1.09 V, a Jsc of 25.07 mA cm^{-2}, and an FF of 84.25 %.

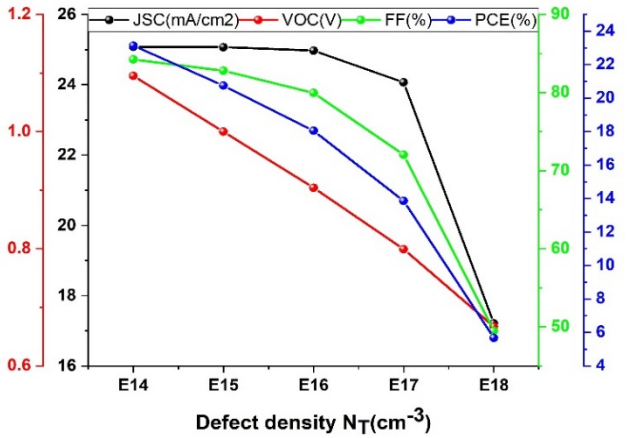

Figure 5. Effect of Defect density N_T (cm^{-3}) on V_{OC}, J_{SC}, FF and PCE

3.5. Influence of Temperature

Understanding the temperature impact on perovskite solar cells is crucial for predicting and enhancing their performance across different conditions. Temperature variations significantly affect the electrical, optical, and structural characteristics of these cells. As temperature rises, perovskite solar cell efficiency typically declines, primarily due to decreased open-circuit voltage (V_{oc}) and fill factor (FF), which collectively reduce overall efficiency. However, higher temperatures can also enhance charge carrier mobility, improving electrical performance. Nonetheless, elevated temperatures may increase recombination rates, shortening charge carrier lifetimes and thereby reducing overall efficiency. Moreover, temperature influences trap state density and activation energy, affecting recombination kinetics [47]. Perovskite materials are sensitive to heat, with excessive temperatures leading to thermal degradation and decreased stability over time. Temperature variations also impact the bandgap of perovskite, altering its optical absorption properties and consequently affecting sunlight absorption and photocurrent. Figures 6.a and 6.b illustrate the impact of temperature on current density–voltage (J–V) features, showing a decrease in V_{oc} with increasing temperature and a decline in short circuit current density (Jsc) alongside increases in V_{OC}, FF, and Power Conversion Efficiency (PCE). Figure 6.c depicts quantum efficiency (QE) functions across different temperatures, crucial for understanding charge collection efficiency and device stability. Changes in QE over time reveal degradation mechanisms, aiding in device improvement. QE also influences the current-voltage (I-V) curve, notably the position of the maximum power point (MPP), crucial for optimal power output. Analysis indicates a mean QE of 87% for a 500 nm absorber layer thickness, with temperature variation enhancing PCE to 21.53 %, accompanied by Voc of 1.02 V, Jsc of 25.32 mA cm^{-2}, and FF of 84.01 %.

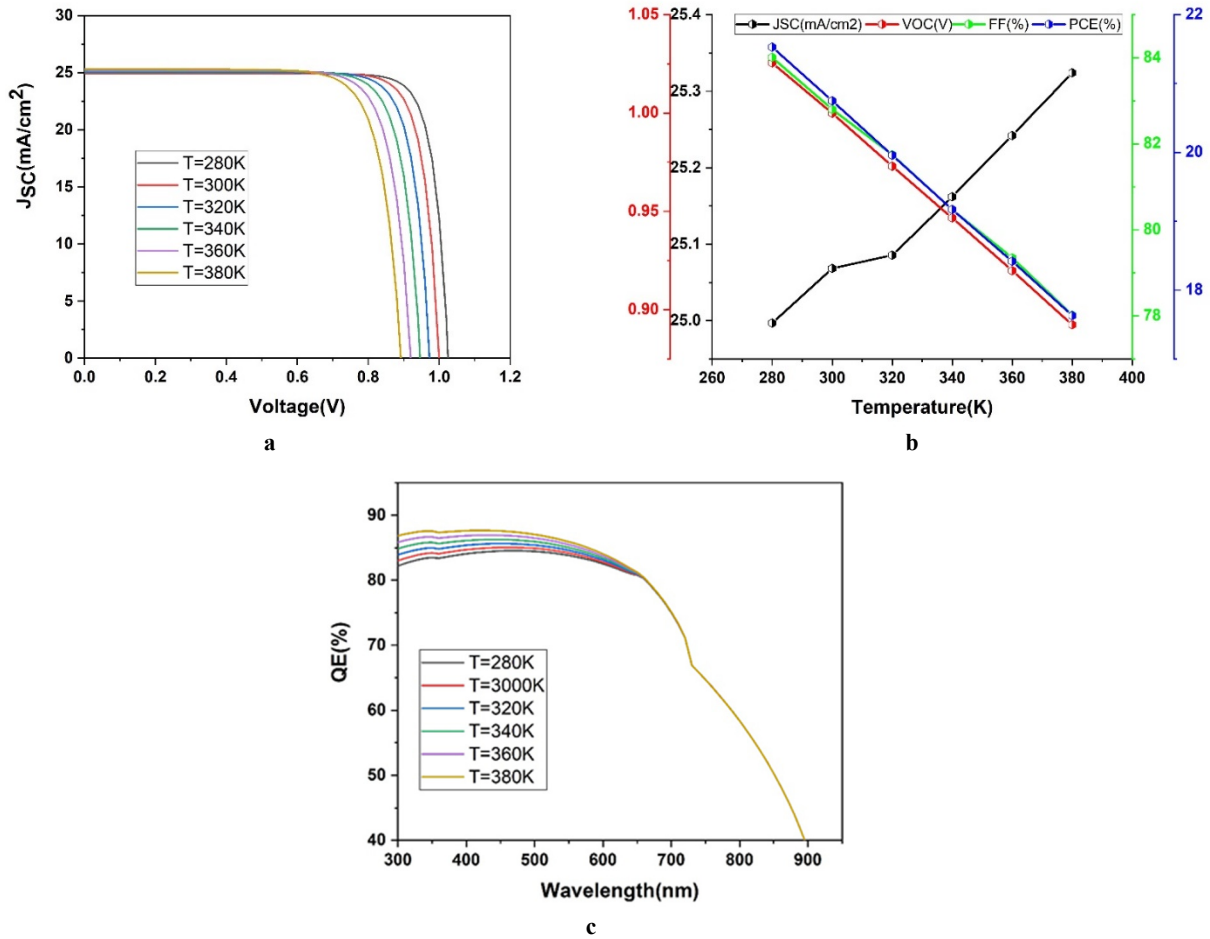

Figure 6. Effect of temperature on J–V (a), V_{OC}, J_{SC}, FF, PCE (b) and QE (c)

3.6 Impact of series resistance and shunt resistance:

In the illustrated Figure 7(a) and (b) successively denotes, Series resistance (R_s) and shunt resistance (R_{sh}) are critical factors affecting the performance of perovskite solar cells, influencing parameters like efficiency and fill factor. Balancing both resistances is vital for optimal performance, with material choices and device architecture playing significant roles. While minimizing series resistance reduces voltage drops along the current path, maximizing shunt resistance allows more current to pass through the active region, enhancing output voltage. Shunt resistance, representing parallel resistance to the current path, reduces current leakage and contributes to increased output voltage and fill factor [48]. Conversely, series resistance, encountered by current flow through cell components, leads to voltage drops and power losses, impacting fill factor and output voltage. As series resistance increases, open circuit voltage (V_{oc}) tends to rise, while shunt

resistance enhancements correlate with increased Voc, fill factor, and power conversion efficiency (PCE). Shunt resistance minimizes voltage losses due to leakage currents, enhancing FF and PCE without affecting short circuit current density (Jsc). The solar cell exhibited a PCE of 20.75%, with a Voc of 0.99 V, Jsc of 25.06 mA cm^{-2}, and FF of 82.8%.

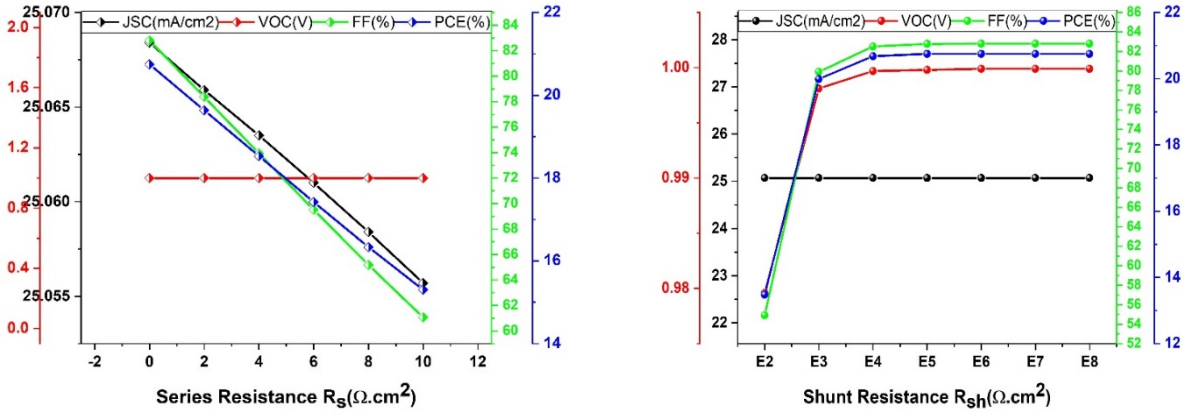

Figure 7. Effect of R_S (a) and R_{Sh} (b) on V_{OC}; J_{SC}; FF; PCE

4. CONCLUSION

In this study, we utilized numerical simulations via the SCAPS-1D platform to assess the performance of perovskite-based solar cells employing $RbGeI_3$ as the absorber material, boasting a wide bandgap of 1.31 eV. By systematically exploring parameters such as temperature, layer thickness, doping, and defects, our aim was to optimize the efficiency of these solar cells, considering their susceptibility to temperature fluctuations. Our findings demonstrate that the proposed configuration effectively extends the absorption spectrum into the near-infrared region, with the thickness of the RbGeI3 layer emerging as a pivotal factor influencing device performance. Analysis revealed that series resistance peaks at 2 $\Omega.cm^2$, while shunt resistance achieves optimal output parameters of up to 10^3 $\Omega.cm^2$. Furthermore, optimization endeavors resulted in a solar cell showcasing a power conversion efficiency of 24.62 %, fill factor of 82.8 %, open circuit voltage of 0.99 V, and short circuit current density of 33.20 mA/cm^2 at a $RbGeI_3$ thickness of 600 nm. This comprehensive numerical investigation not only enhances our understanding of the intricate factors impacting perovskite solar cells but also indicates promising directions for future advancements in the field.

Acknowledgements.
The authors extend their appreciation to Taif University, Saudi Arabia, for supporting this work through project number (TU-DSPP-2024-106)
Funding.
This research was funded by Taif University, Saudi Arabia, Project No. (TU-DSPP-2024-106)

ORCID
Abderrahim Yousfi, https://orcid.org/0000-0003-2071-728X; **Okba Saidani**, https://orcid.org/0000-0003-0507-5581

REFERENCES

[1] L.C. Chen, C.H. Tien, Z.L. Tseng, and J.H. Ruan, "Enhanced efficiency of MAPbI3 perovskite solar cells with $FAPbX_3$ perovskite quantum dots," Nanomaterials, **9**(1), 121 (2019). https://doi.org/10.3390/nano9010121
[2] B. Saparov, *et al*., "Thin-film deposition and characterization of a Sn-deficient perovskite derivative Cs_2SnI_6," Chem. Mater. **28**, 2315–2322 (2016). https://doi.org/10.1021/acs.chemmater.6b00433
[3] B. Lee, *et al*., "Air-stable molecular semiconducting iodosalts for solar cell applications: Cs_2SnI_6 as a hole conductor," J. Am. Chem. Soc. **136**, 15379–15385 (2014). https://doi.org/10.1021/ja508464w
[4] Yousfi, A., and W. Feneniche. "Effect of Graded Double Perovskite for Boosting up the Photovoltaic Output Parameters of Solar Cell: A Numerical Modelling Using SCAPS-1D." Journal of Nano-and Electronic Physics 15.6 (2023). https://doi.org/10.21272/jnep.15(6).06002
[5] B, Sagar, D, Jayan, A, Yousfi et al. "Novel double graded perovskite materials for performance increment of perovskite solar cell using extensive numerical analysis."Physica Scripta 98.9, 095507(2023). https://doi.org/10.1088/1402-4896/aceb97
[6] M. Elbar, S. Tobbeche, S. Chala, O. Saidani, M.N. Kateb, and M.R. Serdouk, "Effect of Temperature on the Performance of CGS/CIGS Tandem Solar Cell," J. Nano- Electron. Phys. **15**(1) 01020 (2023). https://doi.org/10.21272/jnep.15(1).01020
[7] A. Yousfi, O. Saidani, Z. Messai, R. Zouache, M. Meddah, and Y. Belgoumri, "Design and simulation of a triple absorber layer perovskite solar cell for high conversion efficiency," East European Journal of Physics, 4, 137-146 (2023). https://doi.org/10.26565/2312-4334-2023-4-14
[8] S. Shao, J. Liu, G. Portale, H.H. Fang, G.R. Blake, G.H. ten Brink, et al., "Highly reproducible Sn-based hybrid perovskite solar cells with 9% efficiency," Advanced Energy Materials, **8**(4), 1702019 (2018). https://doi.org/10.1002/aenm.201702019
[9] H. Bencherif, and M.K. Hossain, "Design and numerical investigation of efficient $(FAPbI_3)_{1-x}(CsSnI_3)_x$ perovskite solar cell with optimized performances," Sol. Energy, **248**, 137–148 (2022). https://doi.org/10.1016/j.solener.2022.11.012

[10] X. Qiu, *et al*., "From unstable CsSnI3toair-stable Cs_2SnI_6: A lead-free perovskite solar cell light absorber with bandgap of 1.48 eV and high absorption coefficient," Sol. Energy Mater. Sol. Cells, **159**, 227–234 (2017). https://doi.org/10.1016/j.solmat.2016.09.022
[11] M.S. Uddin, M.A. Al Mashud, G.I. Toki, R. Pandey, M. Zulfiqar, O. Saidani, *et al*., "Lead-free Ge-based perovskite solar cell incorporating TiO_2 and Cu_2O charge transport layers harnessing over 25% efficiency," J. Opt. (2023). https://doi.org/10.1007/s12596-023-01570-7
[12] A. Miyata, *et al*., "Direct measurement of the exciton binding energy and effective masses for charge carriers in organic–inorganic tri-halide perovskites," Nat. Phys. **11**, 582–587 (2015). https://doi.org/10.1038/nphys3357
[13] H. Bencherif, *et al*., "Performance enhancement of (FAPbI3)1–x(MAPbBr3)x perovskite solar cell with an optimized design," Micro Nanostruct. **171**, 207403 (2022). https://doi.org/10.1016/j.micrna.2022.207403
[14] Y. Shao, *et al*., "Grain boundary dominated ion migration in polycrystalline organic–inorganic halide perovskite films," Energy Environ. Sci. **9**, 1752–1759 (2016). https://doi.org/10.1039/C6EE00413J
[15] N. Rolston, *et al*., "Engineering stress in perovskite solar cells to improve stability," Adv. Energy Mater. **8**, 1802139 (2018). https://doi.org/10.1002/aenm.201802139
[16] H.L. Zhu, J. Xiao, J. Mao, H. Zhang, Y. Zhao, and W.C.H. Choy, "Controllable crystallization of $CH_3NH_3Sn_{0.25}Pb_{0.75}I_3$ perovskites for hysteresis-free solar cells with efficiency reaching 15.2%," Adv. Funct. Mater. **27**(11), 1605489 (2019). https://dx.doi.org/10.1002/adfm.201605469
[17] M.K. Hossain, *et al*., "Influence of natural dye adsorption on the structural, morphological and optical properties of TiO_2 Based photoanode of dye-sensitized solar cell," Materials Science-Poland, **36**, 93–101 (2017). https://doi.org/10.1515/msp-2017-0090
[18] M.K. Hossain, *et al*., "A comparative study on the influence of pure anatase and Degussa-P25 TiO2 nanomaterials on the structural and optical properties of dye sensitized solar cell (DSSC) photoanode," Optik, **171**, 507–516 (2018). https://doi.org/10.1016/j.ijleo.2018.05.032
[19] H.-S. Kim, *et al*., "Lead Iodide perovskite sensitized all-solid-state submicron thin film mesoscopic solar cell with efficiency exceeding 9%," Sci. Rep. **2**, 591 (2012). https://doi.org/10.1038/srep00591
[20] M.F. Pervez, *et al*., "Influence of total absorbed dose of gamma radiation on optical bandgap and structural properties of Mg-doped zinc oxide," Optik, **162**, 140–150 (2018). https://doi.org/10.1016/j.ijleo.2018.02.063
[21] M.M. Lee, J. Teuscher, T. Miyasaka, T.N. Murakami, and H.J. Snaith, "Efficient hybrid solar cells based on meso-superstructured organometal halide perovskites," Science, **338**, 643–647 (2012). https://doi.org/10.1126/science.1228604
[22] M.N.H. Mia, *et al*., "Influence of Mg content on tailoring optical bandgap of Mg-doped ZnO thin film prepared by sol-gel method," Results Phys. **7**, 2683–2691 (2017). https://doi.org/10.1016/j.rinp.2017.07.047
[23] R. Zouache, I. Bouchama, O. Saidani, L. Djedoui, and E. Zaidi, "Numerical study of high-efficiency CIGS solar cells by inserting a BSF µc-Si: H layer," Journal of Computational Electronics, **21**(6), 1386-1395 (2022). https://doi.org/10.1007/s10825-022-01942-5
[24] A. Mei, *et al*., "A hole-conductor-free, fully printable mesoscopic perovskite solar cell with high stability," Science, **345**, 295-298 (2014). https://doi.org/10.1126/science.1254763
[25] A. Baktash, O. Amiri, and A. Sasani, "Improve efficiency of perovskite solar cells by using Magnesium doped ZnO and TiO_2 Compact layers," Superlattices Microstruct. **93**, 128–137 (2016). https://doi.org/10.1016/j.spmi.2016.01.026
[26] L. Kavan, "Conduction band engineering in semiconducting oxides (TiO_2, SnO_2): Applications in perovskite photovoltaics and beyond," Catal. Today, **328**, 50–56 (2019). https://doi.org/10.1016/j.cattod.2018.10.065
[27] O, SAIDANI, A, YOUSFI, et al. Numerical study of high-performance lead-free CsSnCl3-based perovskite solar cells. Journal of Optics, p. 1-19(2024). https://doi.org/10.1007/s12596-024-01817-x
[28] X.-F. Diao, *et al*., "Study on the property of electron-transport layer in the doped formamidinium lead iodide perovskite based on DFT," ACS Omega, **4**, 20024–20035 (2019). https://doi.org/10.1021/acsomega.9b03015
[29] M.F. Rahman, *et al*., "Concurrent investigation of antimony chalcogenide (Sb_2Se_3 and Sb_2S_3)-based solar cells with a potential WS2 electron transport layer," Heliyon, **8**, e12034 (2022). https://doi.org/10.1016/j.heliyon.2022.e12034
[30] B. Gil, *et al*., "Recent progress in inorganic hole transport materials for efficient and stable perovskite solar cells," Electron. Mater. Lett. **15**, 505–524 (2019). https://doi.org/10.1007/s13391-019-00163-6
[31] Y. Meng, P.P. Sunkari, M. Meilă, and H.W. Hillhouse, "Chemical Reaction Kinetics of the Decomposition of Low-Bandgap Tin–Lead Halide Perovskite Films and the Effect on the Ambipolar Diffusion Length," ACS Energy Letters, **8**(4), 1688-1696 (2023). https://doi.org/10.1021/acsenergylett.2c02733
[32] S. Rafique, S.M. Abdullah, M.M. Shahid, M.O. Ansari, and K. Sulaiman, "Significantly improved photovoltaic performance inpolymer bulk heterojunction solar cells with graphene oxide/PEDOT:PSS double decked hole transport layer," Sci. Rep. **7**, 39555 (2017). https://doi.org/10.1038/srep39555
[33] S. Wang, *et al*., "Role of 4- tert -butylpyridine as a hole transport layer morphological controller in perovskite solar cells," Nano Lett. **16**, 5594–5600 (2016). https://doi.org/10.1021/acs.nanolett.6b02158
[34] C. Liu, *et al*., "Highly stable and efficient perovskite solar cells with 22.0% efficiency based on inorganic-organic dopant-free double hole transporting layers," Adv. Funct. Mater. **30**, 1908462 (2020). https://doi.org/10.1002/adfm.201908462
[35] D. Shin, *et al*., "$BaCu_2Sn(S,Se)_4$: Earth-abundant chalcogenides for thin-film photovoltaics," Chem. Mater. **28**, 4771–4780 (2016). https://doi.org/10.1021/acs.chemmater.6b01832
[36] R. Chakraborty, *et al*., "Colloidal synthesis, optical properties, and hole transport layer applications of Cu_2BaSnS_4 (CBTS) nanocrystals," ACS Appl. Energy Mater. **2**, 3049–3055 (2019). https://doi.org/10.1021/acsaem.9b00473
[37] T. Das, G. Di Liberto, and G. Pacchioni, "Density functional theory estimate of halide perovskite band gap: When spin orbit coupling helps," J. Phys. Chem. C, **126**, 2184–2198 (2022). https://doi.org/10.1021/acs.jpcc.1c09594
[38] M.B. Bechir, and M.H. Dhaou, "Study of charge transfer mechanism and dielectric relaxation of all-inorganic perovskite $CsSnCl_3$," RSC Adv. **11**, 21767–21780 (2021). https://doi.org/10.1039/D1RA02457D
[39] M.S. Ali, S. Das, Y.F. Abed, and M.A. Basith, "Lead-free CsSnCl3 perovskite nanocrystals: Rapid synthesis, experimental characterization and DFT simulations," Phys. Chem. Chem. Phys. **23**, 22184–22198 (2021). https://doi.org/10.1039/D1CP02666F

[40] J. Islam, and A.K.M.A. Hossain, "Semiconducting to metallic transition with outstanding optoelectronic properties of $CsSnCl_3$ perovskite under pressure," Sci. Rep. **10**, 14391 (2020). https://doi.org/10.1038/s41598-020-71223-3
[41] J. Islam, and A.K.M.A. Hossain, "Narrowing band gap and enhanced visible-light absorption of metal-doped non-toxic $CsSnCl_3$ metal halides for potential optoelectronic applications," RSC Adv. **10**, 7817–7827 (2020). https://doi.org/10.1039/C9RA10407K
[42] M.I. Kholil, M.T.H. Bhuiyan, M.A. Rahman, M.S. Ali, and M. Aftabuzzaman, "Effects of Fe doping on the visible light absorption and bandgap tuning of lead-free ($CsSnCl_3$) and lead halide ($CsPbCl_3$) perovskites for optoelectronic applications," AIP Adv. **11**, 035229 (2021). https://doi.org/10.1063/5.0042847
[43] M.I. Kholil, and M.T. H. Bhuiyan, "Effects of Cr- and Mn-alloying on the band gap tuning, and optical and electronic properties of lead-free $CsSnBr_3$ perovskites for optoelectronic applications," RSC Adv. **10**, 43660–43669 (2020). https://doi.org/10.1039/D0RA09270C
[44] O. Saidani, Y. Abderrahim, M. Zitouni, G.S. Sahoo, R. Zouache, M.R. Mohammad, *et al*., "Numerical study of high-performance lead-free $CsSnCl_3$-based perovskite solar cells," Journal of Optics, 1-19 (2024). https://doi.org/10.1007/s12596-024-01817-x
[45] J. Ur Rehman, *et al*., « First-principles calculations to investigate structural, electronics, optical and elastic properties of Sn-based inorganic Halide-perovskites $CsSnX_3$(X = I, Br, Cl) for solar cell applications," Comput. Theor. Chem. **1209**, 113624 (2022). https://doi.org/10.1016/j.comptc.2022.113624
[46] M.H. Ali, *et al*., "Numerical analysis of FeSi2 based solar cell with PEDOT:PSS hole transport layer," Mater. Today Commun. **34**, 105387 (2023). https://doi.org/10.1016/j.mtcomm.2023.105387

ПІДВИЩЕННЯ ЕФЕКТИВНОСТІ ПЕРЕТВОРЕННЯ ЕНЕРГІЇ СОНЯЧНИХ ЕЛЕМЕНТІВ НА ОСНОВІ RbGeI3: ЧИСЕЛЬНИЙ ПІДХІД

Лазхар Лумачі[a], Абдеррахім Юсфі[b], Окба Сайдані[b], Абдулла Саад Альсубайе[c], Уссама Абед[b], Самір Амірі[b], Гіріджа Шанкар Саху[d], М. Расідул Іслам[e]

[a]*Департамент цивільної інженерії, факультет науки і технологій, університет Мохамеда Ель Бачіра Ель Ібрагімі, Бордж Бу Арреріджж-34030, Алжир*
[b]*Лабораторія ETA, департамент електроніки, факультет науки і технологій, університет Мохамеда Ель Бачіра Ель Ібрагімі, Бордж Бу Арреріджж-34030, Алжир*
[c]*Факультет фізики, коледж університету Хурма, Таїфський університет, Таїф 21944, Саудівська Аравія*
[d]*Школа електроніки (SENSE), Веллорський технологічний інститут, Вандалур Келламбаккам, Ченнаї, Таміл Наду 600127, Індія*
[e]*Департамент електротехніки та електронної інженерії, Науково-технологічний університет імені шейха Фоїлатуннеса Муджіба Бангамата, Джамалпур, 2012, Бангладеш*

У поточному дослідженні використовується чисельне моделювання за допомогою платформи SCAPS-1D для дослідження ефективності сонячних елементів на основі перовскіту з RbGeI3, що використовується як поглинаючий матеріал із широкою забороненою зоною 1,31 еВ. Завдяки систематичному дослідженню різних параметрів, включаючи температуру, товщину шару, легування та дефекти, дослідження спрямоване на підвищення ефективності сонячних елементів, враховуючи їхню чутливість до коливань температури. Результати демонструють, що запропонована конфігурація ефективно розширює спектр поглинання в ближню інфрачервону область, при цьому товщина шару RbGeI3 стає критичним фактором, що впливає на продуктивність пристрою. Аналіз показує, що пік послідовного опору досягає 2 $\Omega \cdot см^2$, тоді як опір шунта досягає оптимальних вихідних параметрів до 103 $\Omega \cdot см^2$. Крім того, зусилля з оптимізації призвели до отримання сонячної батареї з ефективністю перетворення потужності 24,62%, коефіцієнтом заповнення 82,8%, напругою холостого ходу 0,99 В і щільністю струму короткого замикання 33,20 мА/см^2 при товщині RbGeI3 0,6 мкм. Це комплексне чисельне дослідження не тільки покращує розуміння складних факторів, що впливають на перовскітні сонячні елементи, але також пропонує багатообіцяючі шляхи для майбутніх досягнень у цій галузі.

Ключові слова: *сонячний елемент; RbGeI3; SCAPS-1D; PSC; PCE*